This document is downloaded from DR-NTU (https://dr.ntu.edu.sg)
Nanyang Technological University, Singapore.

A two-level coordinated voltage control scheme of electric vehicle chargers in low-voltage distribution networks

Wang, Yu; John, Thomas; Xiong, Binyu

2018

Wang, Y., John, T., & Xiong, B. (2019). A two-level coordinated voltage control scheme of electric vehicle chargers in low-voltage distribution networks. Electric Power Systems Research, 168, 218-227. doi:10.1016/j.epsr.2018.12.005

https://hdl.handle.net/10356/143036

https://doi.org/10.1016/j.epsr.2018.12.005

© 2018 Elsevier B.V. All rights reserved. This paper was published in Electric Power Systems Research and is made available with permission of Elsevier B.V.

Downloaded on 25 Apr 2025 09:38:09 SGT

A Two-Level Coordinated Voltage Control Scheme of Electric Vehicle Chargers in Low-Voltage Distribution Networks

Yu Wang[a], Thomas John[b], and Binyu Xiong[c]

[a]*School of Electrical and Electronic Engineering, Nanyang Technological University, Singapore*

[b]*Electrical & Electronic Engineering, Newcastle University, United Kingdom*

[c]*School of Automation, Wuhan University of Technology, China*

Abstract

Nowadays, a growing number of plug-in electric vehicles are charged by electric vehicle chargers (EVCs) in low-voltage (LV) residential networks. Without proper control, the increasing charge demand together with high PV penetration will lead to severe voltage issues. In this paper, a two-level coordinated voltage control scheme of EVCs is proposed for voltage regulation in LV distribution networks. The proposed control scheme includes two coordinated levels to effectively utilize EVCs. In the higher level, the distributed voltage control based on consensus algorithm achieves equal utilization among EVCs for network voltage regulation. In the lower level, the localized power allocator determines the real and reactive power outputs, considering the power limits and charging requirements of each EVC. The entire control scheme ensures that the voltages along the distribution network are within the allowable voltage ranges while avoid affecting the users' charging demand. The proposed control method is evaluated in a LV residential distribution network under various operation conditions. The simulation results validate the effectiveness of the proposed method.

Keywords: Coordinated control, electric vehicle charger, voltage regulation, low-voltage distribution networks.

1. Introduction

1.1 Background

In recent years, the amount of distributed generation (DG) has been increased significantly in distribution networks, which will impose severe stress on network voltages. Especially for low-voltage (LV) residential networks with high penetration of rooftop photovoltaics (PVs) and home charging electric vehicles (EVs), the voltage issues become even worse. The increasing penetration of these DG units in power distribution networks has brought challenges for both planning, operation as well as real-time control [1], [2]. In the daytime, the PV generation may largely exceed the customer load demand. The reverse power flow from customers to the grid can potentially lead to severe voltage rise along the distribution networks [3]. In the evening, the massive charging of EVs can introduce additional load demand, which may result in unacceptable voltage drop issues [4]. The voltage deviations (both voltage rise and drop) beyond acceptable voltage limits will cause electrical equipment failures as well as lifetime degradation.

Distribution networks with a large amount of PV and EV penetrations will increase the number of operation of voltage regulators such as tap-changing transformers and shunt capacitors. The frequent adjustment of the tap/switch of voltage regulators will accelerate their lifetime degradation, and cause additional upgrading cost [5], [6]. Various methods for voltage regulation are proposed to control the real and reactive power outputs of power inverters in distribution networks [7]-[9]. However, the PV real power curtailment method in [7] decreases the efficiency of PV generation. The PV reactive power compensation method in [8] become less effective, due to the high R/X ratio in LV residential networks. Compared to PV inverters, both real and reactive power of a charging EV and its power inverter interface can be utilized within certain charging and capacity limitations [9]. In this paper, the capability of EV and its charger for network voltage regulation will be explored.

1.2 Motivation and Literature Survey

With the fact that private vehicles are parked, on average, 93%–96% of their lifetime, the concept of vehicle-to-grid (V2G) can be implemented [10]. Extensive research has been conducted on the aggregated control, operation, and economics of V2G technology in smart grids [10-14]. For example, the contribution of EVs for power system frequency regulation and inertia has been investigated in [13]. Especially, EVs plugged in the home electric vehicle chargers (EVCs) have much available time and can behave as energy storage devices. By properly selecting the current phase angles of interface power inverters, the EVC can provide inductive or capacitive reactive power [15]. As a result, both the real and reactive power outputs of EVCs can be controlled in compliance with the standard of voltage regulation in distribution networks. In high-density residential areas, EVs are aggregated in EV charging stations and charged simultaneously in a centralized way. The voltage regulation by EV charging stations and EV aggregation have been studied in [16], [17]. But in low-density residential areas, EVs are usually charged by charging outlets at home in a decentralized way. Currently, the coordination of randomized charged EVs and their EVCs, particularly in low-voltage distribution networks, is still lack of investigation. This motivates us to investigate the voltage issues caused by home EV charging as well as voltage regulation methods by coordination of EVCs.

The real-time coordinated control among multiple units is typically achieved by three approaches, i.e. decentralized, centralized and distributed methods. Extensive advanced control approaches have been proposed within these three categories [18]-[22]. In [19], a decentralized voltage regulation strategy based on electric vehicle rapid charger is proposed. From the perspective of power electronics, the reactive power support from electric vehicle charging station is analyzed in [20]. However, the coordination and global optimal operation are hard to achieve by merely applying a decentralized/local control. In [21], a centralized voltage regulation and energy management scheme via V2G/G2V is proposed. In [22], a centralized model predictive control based power dispatch approach of plug-in EVs is introduced. The central controller suffers extensive computation and communication burdens, and centralized control structures are inherently vulnerable to communication failures.

To achieve real-time coordination among different units, the distributed control scheme is adopted without a full central communication architecture. In the distributed control scheme, computation and communication burden are allocated to the distributed controllers, which is more robust to communication failures. The distributed control is suitable for the coordination problems of multiple units and only requires information exchange among neighboring units [23]. Nowadays, the distributed control approaches based on consensus algorithm have been applied to a wide area of electric power system research fields, such as the secondary control of microgrid [24], power system frequency regulation by multiple energy storages [25], real-time economic dispatch among [26] etc..

From the literature survey, it can be found that the coordinated control scheme of both real and reactive power for EVC in LV networks is rarely studied. In this case, the EV will be charged randomly in a residential LV network, which will significantly influence the network voltage without a real-time coordination. Besides, the distributed control to coordinate the utilization of EVC has not been reported yet. Therefore, in this paper, a two-level coordinated voltage control scheme to effectively utilize both real and reactive power provided from EVs and EVCs has been proposed.

1.3 Contributions of This Paper

To fill out the research gap mentioned above, this paper focuses on developing a coordinated control scheme for EVCs to deal with the voltage rise/drop issues caused by high PV and EV penetrations in LV distribution networks. The major contributions are summarized as follows:

1) To describe the behaviors of battery packs on EVs, a lithium-ion battery model based on data fitting curve is developed. This battery model will be used for real-time estimation of the state of charge (SoC) when EV is plugged-into the EVC.

2) A novel two-level coordinated voltage control scheme using EVCs in LV distribution networks is proposed. The higher level obtains the voltage regulation objective by measuring the voltages of critical buses and distributes the control signals to all EVCs via sparse communications. The lower level determines the amount of real and reactive power to be provided by each EVC, considering the operation limits and requirements.

3) The proposed methods have been evaluated with real PV and load profiles in a residential distribution network. The results validate the effectiveness of the proposed method.

This paper is organized as follows. The preliminaries including modeling and assumptions are introduced in Section II. In Section III, the proposed coordinated voltage control method is explained in

detail. Simulation results and discussions are presented in Section IV. Finally, Section V draws the conclusion.

2. Preliminaries

2.1 Lithium-ion Battery Model

An electrical circuit model consisting of a voltage source in series with a resistance is used to characterize the lithium-ion battery, as shown in Figure 1 [27]. In Figure 1, the open-circuit voltage V_{oc} is modeled as a cubic function of SoC, while the internal resistance R_b is modeled as a linear function of SoC. Through fitting the experimental data of the lithium-ion battery in [28], the following equations can be derived:

$$V_{oc} = a_1 SoC^3 + a_2 SoC^2 + a_3 SoC + a_4 \tag{1}$$

$$R_b = \begin{cases} R_{ch} = b_1 SoC + b_2 \\ R_{dis} = b_3 SoC + b_4 \end{cases} \tag{2}$$

where the coefficients a_1-a_4 and b_1-b_4 are shown in Table I, R_{ch} and R_{dis} are the charging and discharging internal resistance respectively. Figure 2 shows the results of the data fitting based on (1), which is compared with experimental data in [28].

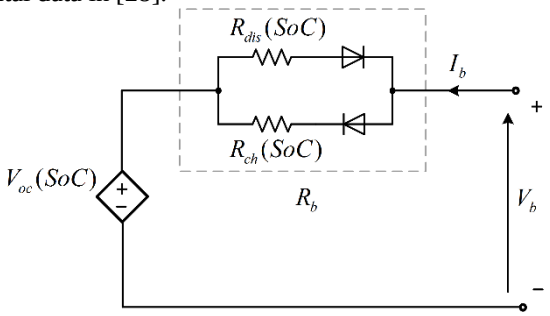

Figure 1: The equivalent circuit model of the lithium-ion battery.

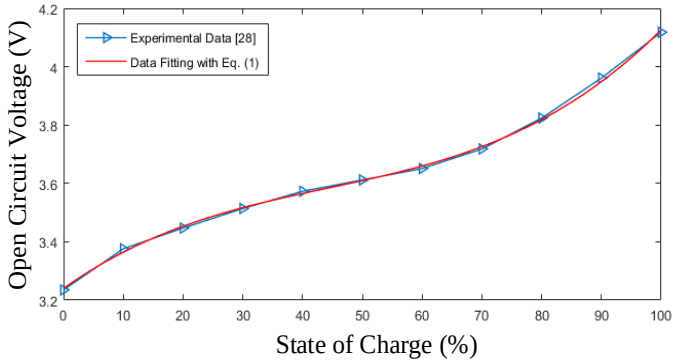

Figure 2: Comparison between data fitting result and experimental data in [28].

According to the electrical model developed above, the battery output voltage V_b can be derived as follows:

$$V_b = V_{oc} + R_b I_b \tag{3}$$

where I_b is the charging/discharging current of the battery.

Table 1: Data fitting results of lithium-ion battery

V_{oc} (V)			
a_1 (V)	a_2 (V)	a_3 (V)	a_4 (V)
1.729	-2.3	1.457	3.24
R_{ch} (mΩ)		R_{dis} (mΩ)	
b_1 (mΩ)	b_2 (mΩ)	b_3 (mΩ)	b_4 (mΩ)
-0.7357	3.957	-1.782	5.191

Based on (1)-(3), the charging and discharging characteristics of the proposed lithium-ion battery can be obtained, as shown in Figure 3 (a) and (b) respectively. It can be observed that the battery output voltage V_b is a function of SoC at a given charging/discharging current I_b. Furthermore, for a certain SoC, V_b is proportional to the charging current, while V_b is inversely proportional to the discharging current.

The SoC of the lithium-ion battery model is estimated using the ampere-hour counting method as:

$$\mathrm{SoC}(k) = \mathrm{SoC}(k-1) + \frac{I_b(k)\Delta t}{C_B} \tag{4}$$

where C_B is the capacity of the lithium-ion battery and Δt is the time interval.

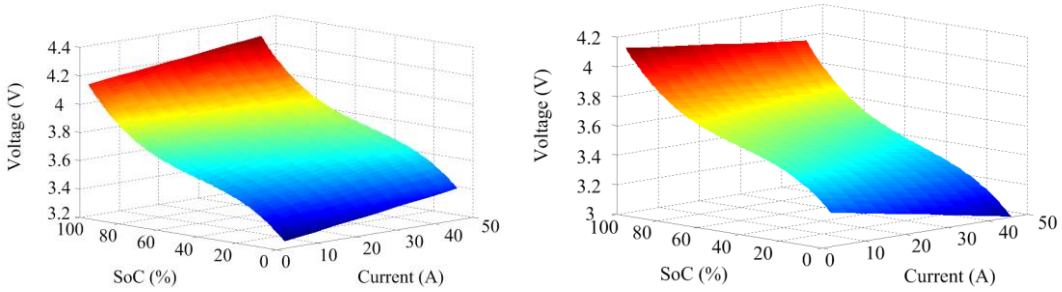

(a) (b)

Figure 3: The charging/discharging characteristic of the lithium-ion battery. (a) charging process. (b) discharging process.

2.2 Assumptions of This Paper

As discussed previously, this paper focuses on the EV charging problem with charging outlets at home (i.e., EVCs) in the community-scale residential area. The studied system is a 400V LV distribution network with multiple EVCs located at certain buses.

The control design and analysis are based on some reasonable assumptions and simplifications, which are listed and discussed as follows:

1) *Types of EVs and EVCs*. The EVs are considered as Nissan Leaf with a storage capacity of 24kWh, which has a battery pack consisting of 120 lithium-ion battery cells connected in series [29]. The EVCs are 230V/16A level II battery charger with 3.6kVA charging power rating [30]. The same power rating is assumed to be valid for the discharging process in V2G mode.
2) *Modeling of EVs and EVCs*. As the focus of this research is on the voltage issues in distribution networks caused by the charging of EV, the EVC is modelled as a controlled current source. The simplification is widely applied when analyzing PV/EV penetrations in distribution networks [20], [31]. The EVs are modeled as battery pack mentioned above. In addition, the EV will operate in the SoC linear range of the lithium-ion battery characteristic, which is between 10% and 90% of SoC, to avoid depletion or saturation of EV's battery pack.
3) *EV charging behavior*. Once an EV is plugged in the EVC, the EV user's individual information including arrival time, estimated departure time and initial SoC is recorded. All EVs will be charged to the desired SoC of 80% before departure. This is preferable from the EV users' point of view that the EV will have sufficient energy for the next trip.

3. Proposed Voltage Control Scheme

Based on the preliminaries, a two-level coordinated voltage control scheme of EVCs is proposed, which includes localized power allocator and distributed voltage control. The functionality of the power allocator (lower level) is to determine whether the EV works in V2G mode or maximum power charging mode based on local information. If the EV is in V2G mode, the EV will participate in the distributed voltage control (higher level) when there is a voltage limit violation at critical buses. Otherwise, the EV is charged by the maximum power rating of the EVC.

The control structure of the proposed voltage regulation method is shown in Figure 4. In Figure 4, the voltage of the critical bus is measured by the virtual leader to initiate the voltage regulation. In the higher level, information state u of each EVC is updated with the signals received from adjacent EVCs. Then the power allocator determines how much real and reactive power can be provided by each EVC in the lower level. The details of the proposed voltage regulation method are explained in the following

subsections.

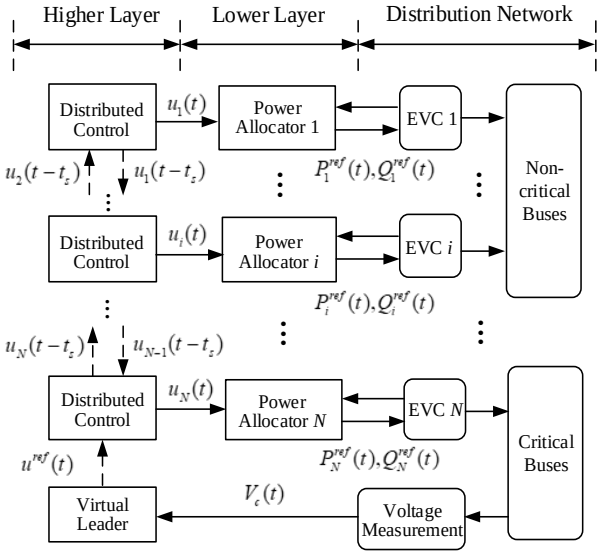

Figure 4: Configuration of the proposed voltage control scheme.

3.1 Higher Level: Distributed Voltage Control

The higher level of the proposed method is to coordinate EVCs in a distributed way for voltage regulation in LV distribution networks. The distributed control is achieved by the consensus algorithm which shares the information state among all available units through communication links between them. The information state is initiated by the virtual leader which measures the information of the critical bus [31]. With the information state provided by the virtual leader, the distributed control will determine the information state u for each EVC. The number of EVCs is represented by i=1, 2, … , N.

For a radial distribution feeder without laterals, the last bus usually has the highest/lowest voltage in this feeder, which is defined as a critical bus. For a distribution network with multiple laterals, the last bus of each lateral may have the highest/lowest voltage of the network. Therefore, several critical buses are selected as virtual leaders to initiate distributed control.

The information state of the virtual leader u^{ref} at a critical bus is updated as follows:

$$u^{ref}(t)=\begin{cases} u^{ref}(t-t_s)+k_1(V_c(t)-1.05V_0) & V_c(t)>1.05V_0 \\ u^{ref}(t-t_s) & 1.05V_0>V_c(t)>1.03V_0 \\ 0 & 1.03V_0>V_c(t)>0.97V_0 \\ u^{ref}(t-t_s) & 0.97V_0>V_c(t)>0.95V_0 \\ u^{ref}(t-t_s)+k_2(V_c(t)-0.95V_0) & V_c(t)<0.95V_0 \end{cases} \quad (5)$$

where V_c is the voltage of the critical bus, V_0 is the voltage of the transformer bus, which is set to 1.0 p.u. in this paper. Parameters k_1 and k_2 are the control gains, which affect the convergence speed and control accuracy of the distributed control, and t_s is the sampling interval.

The distribution systems are normally allowed a maximum voltage deviation of 5%-10% (depending on national standards) from the secondary of the transformer to the customer end [3]. In this paper, the upper and lower voltage references in (5) are chosen as $1.05V_0$ and $0.95V_0$ respectively. Thus, the voltage of the distribution network will be regulated within allowable voltage range if all EVCs can provide enough real and reactive power. According to (5), if the voltage of the critical bus V_c goes beyond $1.05V_0$, u^{ref} will start to increase. If the voltage of the critical bus V_c drops below $0.95V_0$, u^{ref} will start to decrease. If V_c is between $1.03V_0$ and $0.97V_0$, u^{ref} will become 0. Otherwise, u^{ref} will keep the value of the previous step.

The information state u^{ref} of the virtual leader is then communicated to each EVC through communication links. The instantaneous communication graph can be represented by the following matrix:

$$S(t)=\begin{bmatrix} s_{11}(t) & s_{12}(t) & \cdots & s_{1N}(t) \\ s_{21}(t) & s_{22}(t) & \cdots & s_{2N}(t) \\ \vdots & \vdots & \ddots & \vdots \\ s_{N1}(t) & s_{N2}(t) & \cdots & s_{NN}(t) \end{bmatrix} \tag{6}$$

where s_{ij} denotes the communication link between the ith and jth EVCs. $s_{ii} = 1$ for all i, $s_{ij} = 1$ if the information state of the jth bus is received by the ith bus at time t, and $s_{ij} = 0$ if otherwise. In this paper, it is assumed that all EVCs only communicate with their adjacent neighbours, which means all $s_{(i)(i-1)} = 1$ and $s_{(i)(i+1)} = 1$. The communication graph can be known by each EVC as a prior knowledge.

During some periods, the plug-in EVs and the associated EVCs may change their charging behaviours and will not join the network voltage regulation. Under this condition, the global communication graph will change due to the addition and removal of certain EVCs. Hence, a distributed graph discovery algorithm is proposed to determine the matrix S and the number of EVCs N which participates in the voltage regulation. This algorithm is also applicable when there is a communication failure or when new EVCs participate in voltage regulation.

It is assumed that each EVC i is assigned a unique identifier $ID(i)$, and $G_i(k)$ denotes the neighbor set obtained by EVC i. The graph discovery algorithm is designed as follows:

1) At $k = 0$, each EVC i initializes the set $G_i(k)$ as $G_i(k) = \{ID(i)\ [ID(j)]\}$, where $ID(j)$ is identifier of the EVC j which has communication link with EVC i. $G_i(0)$ will be sent to all its neighbors EVC j.
2) For each step $k \geq 1$, EVC i updates its set $G_i(k)$ as $G_i(k) = G_i(k-1) \bigcup G_j(k-1)$.
3) If $G_i(k) = G_i(k-1)$, then EVC i stops exchanging information with its neighbors, and this time instant is recorded as K_1. Otherwise, go to step 2.
4) Finally, the total EVC number N can be extracted by counting the number of elements in set $G_i(K_1)$, which is also the dimension of matrix S. The identifier of EVC which participates in the voltage regulation will be known by each EVC.

With information state of virtual leader u^{ref} and communication graph S obtained above, the information state u_i for the EVC i is updated as follows:

For EVC i at critical bus,

$$u_i(t) = \sum_{j \neq i}^{N} d_{ij}(t) u_j(t - t_s) + d_{ii}(t) u^{ref}(t) \tag{7}$$

For EVC i at non-critical bus,

$$u_i(t) = \sum_{j=1}^{N} d_{ij}(t) u_j(t - t_s) \tag{8}$$

where $d_{ij}(t)$ is the (i, j) entry of a row stochastic matrix (i.e., row sum of 1) $D(t)$ which can be found in each discrete time data exchange as follows:

$$d_{ij}(t) = \frac{\omega_{ij} s_{ij}(t - t_s)}{\sum_{j=1}^{N} \omega_{ij} s_{ij}(t - t_s)} \tag{9}$$

where the weights ω_{ij} are set to 1 in this paper to share the required power equally among distributed EVCs and s_{ij} are the entries of the communication matrix $S(t)$, as given in (6).

3.2 Lower Level: Localized Power Allocator

The lower level of the proposed method is to determine the real and reactive power outputs of each EVC considering the operation limits and requirements. As mentioned before, the voltage regulation objective of the higher level must be achieved within the power limits of each EVC and the SoC limits of corresponding plug-in EV, which can be described by (10) and (11) respectively

$$-S^{max} \leq S_{EVC}(t) \leq S^{max} \tag{10}$$

$$SoC^{min} < SoC(t) < SoC^{max} \tag{11}$$

The operation requirement is that the plug-in EV needs to be charged to the desired SoC level of 80% before leaving. Therefore, the power allocator needs to determine the mode of operation of the EV. In V2G mode, the EV can participate in the voltage regulation and work as an energy storage device. The real power of the EV can be utilized depending on the information state and real-time SoC. While in maximum power charging mode, the EV cannot participate in the voltage regulation and should work as a constant power load in the system.

The following algorithm is developed to determine whether the EV plugged in EVC i will work as V2G mode or maximum power charging mode.

1) At $k = 1$, the plug-in EV's current SoC value $SoC(1)$ and estimated departure time t_d are recorded.
2) For each step $k \geq 1$, with SoC information $SoC(k)$ and (1)-(3) of battery model, the maximum charging current I^{max} at time instant k is derived as follows:

$$I^{max}(k) = \frac{1}{2R_b(k)}(V_{oc}(k) - \sqrt{V_{oc}(k)^2 - 4R_b(k)P^{max}}) \tag{12}$$

where V_{oc} and R_b can be calculated by substituting $SoC(k)$ into (1) and (2).

3) With maximum charging current obtained by (12), $SoC(k+1)$ of the next step can be estimated as follows:

$$SoC(k+1) = SoC(k) - \frac{I^{max}(k)\Delta t}{C_B} \tag{13}$$

4) If $SoC(k) \geq 80\%$, this time instant is recorded as K_2, and go to the next step. Otherwise, go back to step 2. $K_2\Delta t$ is the charging time required in which the EV is charged from $SoC(1)$ to 80% with maximum charging power.
5) Compare $K_2\Delta t$ with the time left for the EV before leaving $(t_d - t)$.
   If $K_2\Delta t \geq (t_d - t)$, the EV will work in maximum power charging mode.
   If $K_2\Delta t < (t_d - t)$, the EV will work in V2G mode.

In the above algorithm, the minimum charging time of the EV (i.e., the charging time with the maximum charging power) is estimated through steps 1-4. The EV's minimum charging time is compared with the time left before leaving to determine the mode of operation in step 5.

If the EV works in V2G mode, the real power output of the EVC is controlled by the u_i considering the power limits and SoC limits as follows:

$$P_i^{ref}(t) = \begin{cases} P^{max} & u_i(t) \geq 1 \,\&\, SoC_i(t) > 0.1 \\ u_i(t)P^{max} & 0 \leq u_i(t) < 1 \,\&\, SoC_i(t) > 0.1 \\ u_i(t)P^{max} & -1 \leq u_i(t) < 0 \,\&\, SoC_i(t) < 0.9 \\ -P^{max} & u_i(t) < -1 \,\&\, SoC_i(t) < 0.9 \\ 0 & otherwise \end{cases} \tag{14}$$

If the EV works in maximum power charging mode, the EV must be charged with maximum charging power.

The reactive power output of each EVC will be utilized only when the real power output of each EVC is not enough for the voltage regulation. The reactive power output of each EVC is controlled by the u_i and reactive power limits as follows:

$$Q_i^{ref}(t) = \begin{cases} Q_i^{max}(t) & u_i(t) \geq 2 \\ (u_i(t)-1)Q_i^{max}(t) & 1 \leq u_i(t) < 2 \\ 0 & -1 \leq u_i(t) < 1 \\ (u_i(t)+1)Q_i^{max}(t) & -2 \leq u_i(t) < -1 \\ -Q_i^{max}(t) & u_i(t) < -2 \end{cases} \tag{15}$$

The maximum reactive power which can be provided by each EVC is determined by the power capacity and real power output of the EVC as follows:

$$Q_i^{max}(t) = \sqrt{(S^{max})^2 - P_i^{ref}(t)^2} \tag{16}$$

Finally, the power output of each EVC will be provided according to P_i^{ref} and Q_i^{ref}.

4. Results and Discussions

4.1 Test System

A 17-bus distribution network is implemented in Matlab/Simulink to verify the performance of the proposed voltage regulation method. The configuration of the test distribution network is shown in Figure 5. It is assumed that there are both PV generation and load demand at each bus, and totally 10 buses are installed the EVCs in the distribution system. The communication links between adjacent EVCs are represented by dot line, as shown in Figure 5. The residential distribution network is connected to the utility gird through a 1MVA, 22/0.4kV transformer. The phase voltage at the secondary of the transformer is set as 230V (1.0p.u.). The bus to bus distances of the main feeder, laterals 1, 2 and 3 are 50m, 100m, 40m, and 30m respectively. Buses 6, 12 and 16 are the critical buses which potentially have the highest voltage in the system. The parameters of the simulation system are given in Table 2. To evaluate the proposed voltage regulation method in a realistic environment, the real solar PV and residential load profiles are used in the simulation. The PV output data are collected every 5 minutes using the GL 130 PV module in summer of 2014 at Clean Energy Research Laboratory, Nanyang Technological University, Singapore. The load profiles are typical residential load profiles, which are presented in [32]. The PV and load profiles used in this paper are shown in Figure 6. The original load data (in p.u.) obtained from [32] is scaled up 1.8 for heavy load and 1.4 for light load conditions. In addition, this study focuses on a distribution network in one community-scaled area. Therefore, identical PV and load profiles are applied for each bus. Two test cases are conducted and discussed in the following subsections. Table 3 shows the plug-in EV information of EVCs for two test scenarios.

1.

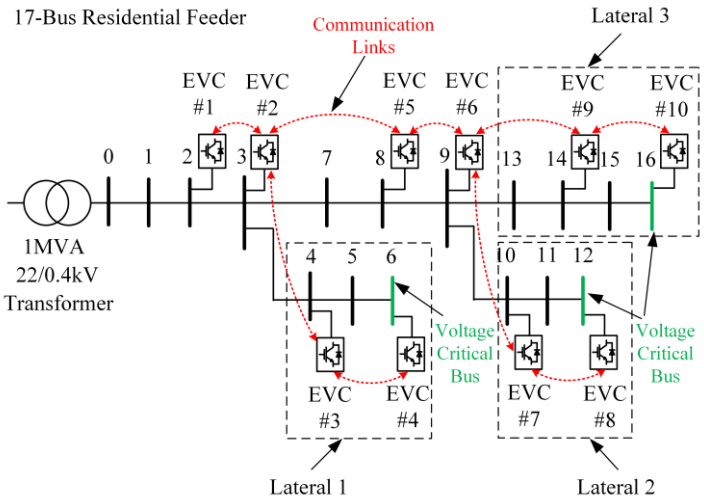

Figure 5: Configuration of the 17-bus residential distribution network.

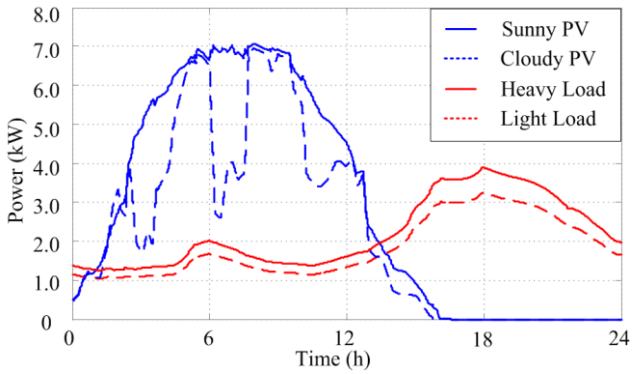

Figure 6: PV generation and load profiles for the simulation study.

Table 2: Parameters of the simulation system

Parameter	Value
System Frequency	50Hz
MV/LV Transformer Size	1MVA, 22/0.4kV
Line Impedence	0.549 + j0.072Ω/km
EVC Rating (S^{max})	3.6kVA
Nissan Leaf EV Capacity	24kWh
SoC Limits (SoC^{min}, SoC^{max})	10%, 90%
Distributed Control (k_1, k_2)	0.01, 0.01
Voltage Reference (V^{low}, V^{up})	0.95p.u., 1.05p.u.

Table 3: EV charging behavior of each EVC

EVC ID (i)	EV Information		
	Initial SoC (%)	Arrival Time (h)	Departure Time (h)
EVC #1	50	16:00	06:00
EVC #2	45	17:00	07:00
EVC #3	40	18:00	08:00
EVC #4	35	19:00	08:30
EVC #5	30	20:00	07:30
EVC #6	25	21:00	06:30
EVC #7	20	10:00	18:00
EVC #8	30	12:00	20:00
EVC #9	40	14:00	22:00
EVC #10	40	08:00	07:59

4.2 Test Case 1

The first test case demonstrates the proposed method under sunny PV generation and light load condition. The voltage profiles with uncoordinated EV charging (i.e., charging with maximum power once plugged in) are shown in Figure 7 (a). The voltage profiles with the proposed voltage regulation method are shown in Figure 7 (b). As shown in Figure 7 (a), there are both bus voltage rise and drop beyond the allowable voltage range [0.95p.u., 1.05p.u.] in this distribution network. From 10:15h to 15:05h in the daytime, buses 8-16 violate the upper voltage reference 1.05p.u. and the highest voltage is 1.067p.u. at bus 16 at 14:00h. From 18:30h to 22:30h in the evening, buses 8-16 violate the lower voltage reference 0.95p.u. and the lowest voltage is 0.941p.u. at bus 16 at 20:00h. As shown in Figure 7 (b), with the proposed voltage regulation method applied for each EVC, the voltages can be regulated within the allowable voltage range. The real and reactive power outputs and the SoC profile of each EVC during the operation period are shown in Figure 8. It should be mentioned that in Figure 8, positive values mean absorption of power by the EVC, while negative values mean the injection of power by the EVC.

The simulation results of test case 1 are further explained in time sequences as follows:

1) 08:00h≤t<10:20h. Although PV generation is larger than the load demand during this period, the voltages of all buses are still below 1.05p.u. Therefore, no voltage regulation is needed during this period. As shown in Figure 7, the real and reactive power outputs of each EVC remain 0.

2) 10:20h≤t<13:10h. The PV generation increases significantly during the midday and becomes much larger than the load demand. The voltages of critical buses exceed 1.05p.u. at 10:20h and the proposed voltage regulation method is initiated. The information state u_i is between 0 and 1 during this period and the real power outputs of EVCs # 7, 8 and 10 are utilized for voltage regulation.

3) 13:10h≤t<15:20h. As PV generation increases further, the real power charged by each EVC is not enough for voltage regulation. The information state u_i increases between 1 and 2 and EVCs #1-6 which cannot absorb real power begin to absorb reactive power for voltage regulation. Moreover, as shown in Table 3, an EV is plugged in EVC #9 at 14:00h. Therefore, real power instead of reactive power is absorbed at EVC #9 for voltage regulation from 14:00h to 15:20h.

4) 15:20h≤t<18:40h. Although PV generation decreases significantly, the voltages of critical buses drop below 1.03p.u. but still above the lower voltage reference 0.95p.u. Therefore, voltage regulation is not needed during this period. In addition, as the SoC of the EV plugged in EVC #7 is above 80%, there is no mode change before its leaving at 18:00h.

5) 18:40h≤t<23:05h. The voltages of critical buses drop below 0.95p.u. at 18:40h. The information state u_i decreases between -1 and 0 during this period and the real power outputs of all available EVCs

are enough for voltage regulation. As EVs plugged in EVC #8 and EVC #9 will leave during this period, they need to be charged with maximum charging power until their SoCs reaching 80% before their leaving, as shown in Figure 8.

6) 23:05h≤t≤24:00h. As the load demand decreases during this period, the voltages of critical buses increase above 0.97p.u. Therefore, no voltage regulation is required during this period.

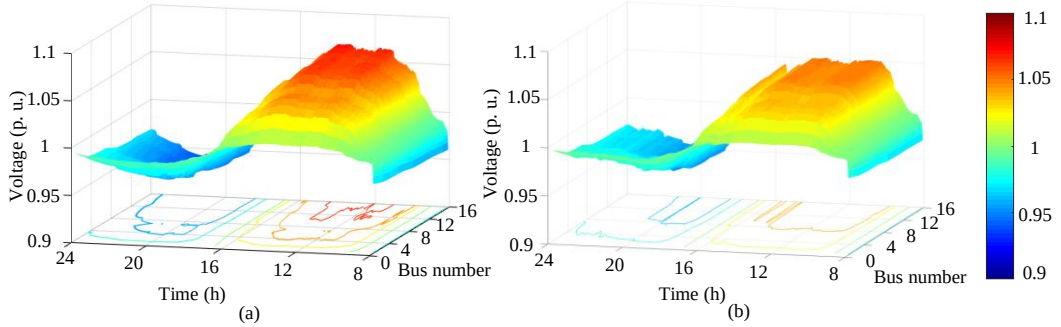

Figure 7: Voltage profiles of the distribution network in test case 1. (a) Uncoordinated EV charging. (b) Proposed voltage regulation method.

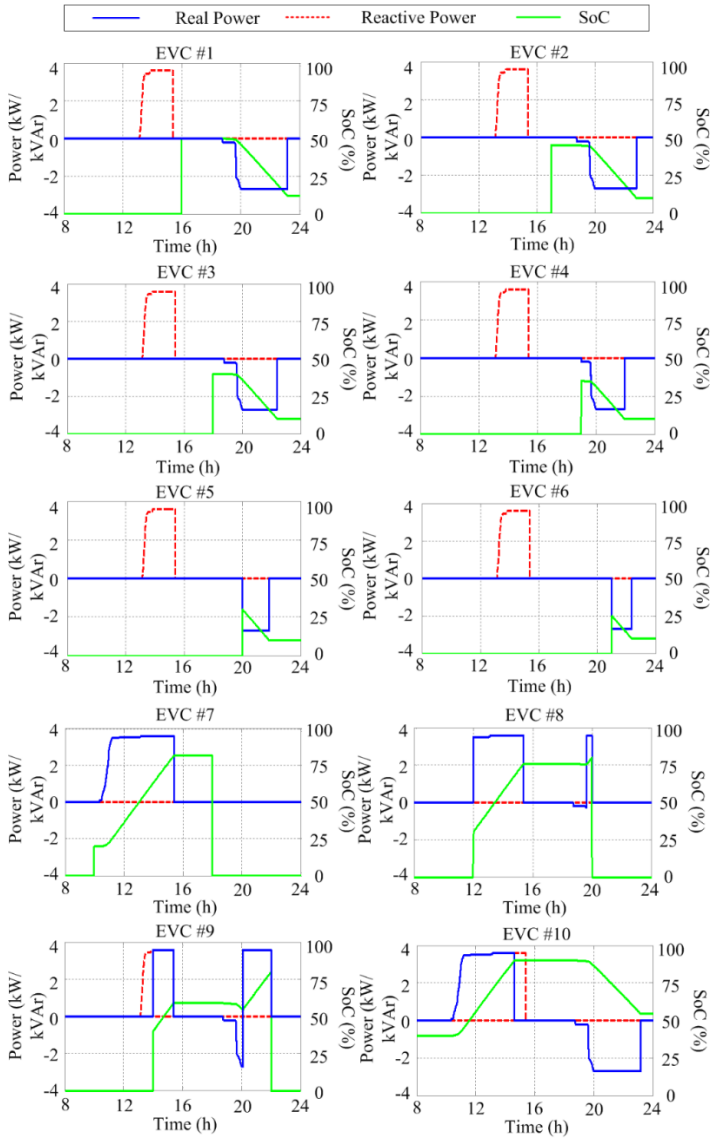

Figure 8: Real and reactive power outputs and SoC profile of each EVC.

4.3 Test Case 2

The second test case demonstrates the proposed method under cloudy PV generation and heavy load condition. For comparison, the voltage profiles with uncoordinated EV charging are shown in Figure 9 (a). The voltage profiles with the proposed voltage regulation method for test case 2 are shown in Figure 9(b). As shown in Figure 9(a), there are still bus voltage rise and drop issues in the distribution network. Due to the cloudy weather condition in the daytime, there are some large voltage variations and the voltage rise problem becomes less severe than test case 1. In the evening, the voltage drop problem becomes more severe due to the heavy load demand and the lowest voltage is 0.93p.u. at bus 16 at 20:00h. As shown in Figure 9(b), with the proposed method applied for each EVC, the voltages can be regulated within the allowable voltage range. The real and reactive power outputs and the SoC profile of each EVC during the operation period are shown in Figure 10.

The simulation results of test case 2 are further explained in time sequences as follows:

1) *08:00h≤t<11:10h.* Although PV generation is larger than the load demand, the voltages of all buses are below 1.05p.u. Therefore, no voltage regulation is needed.
2) *11:10h≤t<14:40h.* As PV generation increases in the midday, the voltages of critical buses are beyond 1.05p.u. at 11:10h. The real power outputs of EVCs #7, 8, 9 and 10 are utilized for voltage regulation during this period, as shown in Figure 10. The voltage regulation stops working due to the large PV variation from 12:00h to 13:05h.
3) *14:40h≤t<18:25h.* The voltages of critical buses drop below 1.03p.u. but still above the lower voltage reference 0.95p.u. The voltage regulation is not applied during this period. In addition, the SoC of the EV plugged in EVC #7 is not fully charged during the daytime, so the EV changes to maximum power charging mode at 15:25h and is charged to 80% of the SoC at 18:00h before leaving.
4) *18:25h≤t<19:50h.* The voltages of critical buses drop below 0.95p.u. at 18:25h. EVCs #1, 2, 3, 4, 9 and 10 begin to inject real power for voltage regulation. The real power outputs of all available EVCs are enough for voltage regulation during this period.
5) *19:50h≤t<22:50h.* As the EV plugged in EVC #9 will leave at 22:00h, the compulsive charging increases the load demand. The real power discharged by available EVCs are not enough for voltage regulation. EVCs which cannot inject real power begin to inject reactive power. The reactive power instead of real power of EVCs #1-6 is utilized for voltage regulation when plug-in EV is fully discharged.
6) *22:50h≤t≤24:00h.* As the load demand decreases significantly during this period, the voltages of critical buses increase above 0.97p.u. Therefore, voltage regulation is no longer needed during this period.

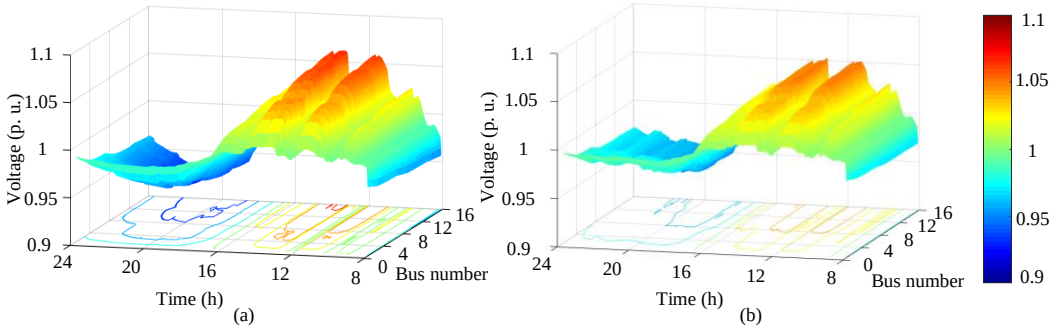

Figure 9: Voltage profiles of the distribution network in test case 2. (a) Uncoordinated EV charging. (b) Proposed voltage regulation method.

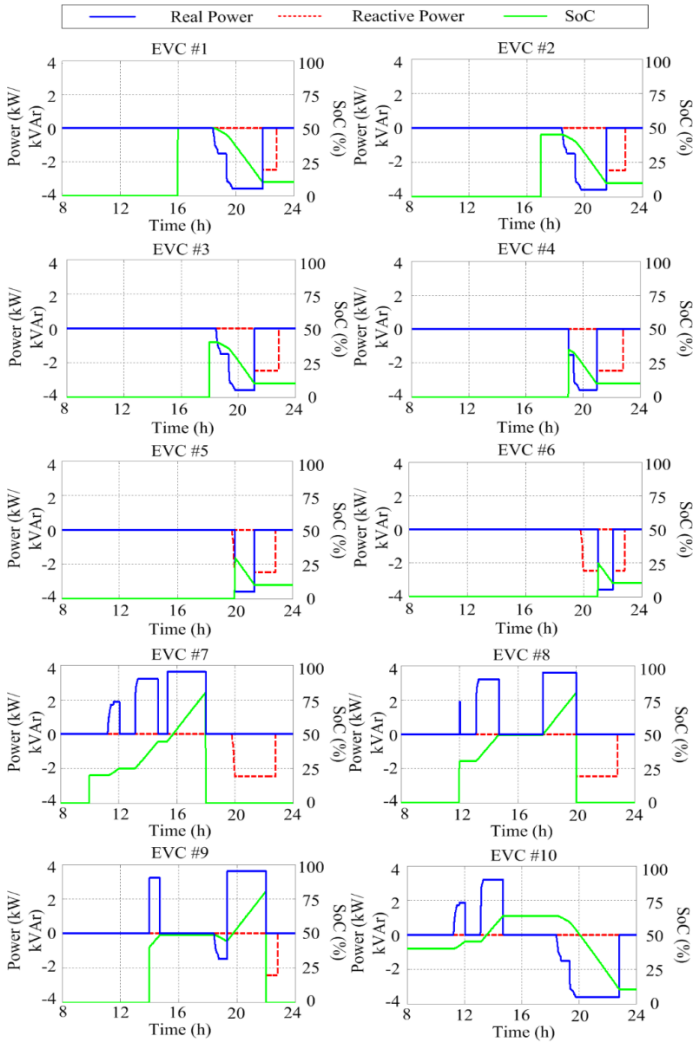

Figure 10. Real and reactive power outputs and SoC profile of each EVC.

4.3 Discussions

Validation and Effectiveness: In summary, the simulation results validate the effectiveness of the proposed method in both cases. It can be found that the proposed method can deal with some of the worst scenarios such as light load/sunny PV and heavy load/cloudy PV. This indirectly validates the proposed method will also take effect for normal operation conditions. Typical EV charging behavior in Table 3 is considered in this paper. As shown in Figure 8 and 10, all EVCs respond in an expected manner for network voltage regulation according to the proposed method. Particularly, the EVC #10 with a whole day plug-in EV functions like a grid energy storage system. For other EVCs, the real power will be firstly used when it is available. The reactive power will be used if the EVs is not available (e.g. fully charged/discharged or absent). The proposed method can always ensure that the network voltages are regulated within the limits as long as there are enough real and reactive power reserves from EVCs. However, additional voltage adjustment methods such as tap changing transformers and switched capacitors are also applicable for a supplement if the power from EVCs is not enough to handle the network voltage regulation.

Future Works: There are still several parts which can be further improved in future work. Firstly, the state-of-health (SoH) is not considered in the lithium-ion battery modelling in this research. However, due to the limited life cycle of the lithium-ion battery, the SoH and capacity fading are important issues to be considered for long time operation. Secondly, the EV user data is considered as a given information in this research. In future research, probability-based model can be built to estimate the SoCs of the EVs and the parking/charging time of the EV users. Furthermore, the research scope is limited to the voltage regulation and EV charging problem in a low-density residential area. For different areas (commercial

or residential), the time and amount of EV charging could be quite different. The real-time voltage regulation through V2G needs to consider EV management strategies as well.

5. Conclusions

In this paper, EVCs have been utilized to regulate the voltages in LV distribution networks. A lithium-ion battery model has been developed for SoC estimation. A coordinated voltage control method which includes two control levels has been proposed to calculate the power outputs of EVCs during daily operation. The power outputs of the EVCs are determined by both distributed voltage control and localized power allocator. A 17-bus distribution network has been implemented in Matlab/Simulink to validate the performance of the proposed method. Based on the information state generated by distributed voltage control, the power allocator of each EVC can determine the real and reactive power outputs to realize voltage regulation. The simulation results have shown that the voltages along the distribution network are regulated within allowable voltage ranges under considered operational conditions. The advanced control methodologies considering capacity fading, stochastic EV charging behaviors, and more application scenarios will be further investigated for network voltage regulation by EVCs.

References

[1] P. S. Georgilakis, and N. D. Hatziargyriou. "A review of power distribution planning in the modern power systems era: Models, methods and future research," *Electric Power Systems Research*, vol. 121, pp. 89-100, Apr. 2015.

[2] N. Mahmud, and A. Zahedi. "Review of control strategies for voltage regulation of the smart distribution network with high penetration of renewable distributed generation," *Renewable and Sustainable Energy Reviews*, vol. 64, pp. 582-595, Oct. 2016.

[3] R. Tonkoski, D. Turcotte, and T. H. M. El-Fouly, "Impact of high PV penetration on voltage profiles in residential neighborhoods," *IEEE Trans. Sustainable Energy*, vol. 3, no. 3, pp. 518-527, Jul. 2012.

[4] K. Clement-Nyns, E. Haesen, and J. Driesen, "The impact of charging plug-in hybrid electric vehicles on a residential distribution grid," *IEEE Trans. Power Systems*, vol. 25, no. 1, pp. 371-380, Dec. 2009.

[5] M. E. Elkhatib, R. El Shatshat, and M. M. A. Salama, "Optimal control of voltage regulators for multiple feeders," *IEEE Trans. Power Delivery*, vol. 25, no. 4, pp. 2670-2675, Oct. 2010.

[6] X. H. Liu, A. Aichhorn, L. M. Liu, and H. Liu, "Coordinated control of distributed energy storage system with tap changer transformers for voltage rise mitigation under high photovoltaic penetration," *IEEE Trans. Smart Grid*, vol. 3, no. 2, pp. 897-906, Feb. 2012.

[7] R. Tonkoski, L. A. C. Lopes, and T. H. M. El-Fouly, "Coordinated active power curtailment of grid connected PV inverters for overvoltage prevention," *IEEE Trans. Sustainable Energy*, vol. 2, no. 2, pp. 139-147, Apr. 2011.

[8] P. Jahangiri and D. C. Aliprantis, "Distributed volt/Var control by PV inverters," *IEEE Trans. Power Systems*, vol. 28, no. 3, pp. 3429-3439, Aug. 2013.

[9] D. Sbordone, et al. "EV fast charging stations and energy storage technologies: A real implementation in the smart micro grid paradigm," *Electric Power Systems Research*, vol. 120, pp. 96-108, Mar. 2015.

[10] H. Turton and F. Moura, "Vehicle-to-grid systems for sustainable development: An integrated energy analysis," *Technological Forecasting and Social Change*, vol. 75, no. 8, pp. 1091-1108, Oct. 2008.

[11] R. J. Bessa, and Manuel A. Matos. "Economic and technical management of an aggregation agent for electric vehicles: a literature survey," *European transactions on electrical power*, vol. 22, no .3, pp. 334-350, Apr. 2012.

[12] M. A. Ortega-Vazquez, F. Bouffard, and V. Silva. "Electric vehicle aggregator/system operator coordination for charging scheduling and services procurement," *IEEE Trans. Power Systems*, vol. 28, no. 2, pp. 1806-1815, May 2013.

[13] M. H. Amini, A. Kargarian, and O. Karabasoglu, "ARIMA-based decoupled time series forecasting of electric vehicle charging demand for stochastic power system operation," *Electric Power Systems Research*, vol. 140, pp. 378-390, Nov. 2016.

[14] P. R. Almeida, F. J. Soares, and J. P. Lopes. "Electric vehicles contribution for frequency control with inertial emulation," *Electric Power Systems Research*, vol. 127, pp. 141-150, Oct. 2015.

[15] M. Pinto, V. Monteiro, H. Goncalves, and J. L. Afonso, "Vehicle-to-grid reactive power operation using plug-in electric vehicle bidirectional offboard charger," *IEEE Trans. Industrial Electronics*, vol. 61, no. 12, pp. 6778-6784, Mar. 2014.
[16] F. Marra, G. Y. Yang, C. Træholt, E. Larsen, et al., "EV charging facilities and their application in LV feeders with photovoltaics," *IEEE Trans. Smart Grid*, vol. 4, no. 3, pp. 1533–1540, Aug. 2013.
[17] M. Singh, P. Kumar, and I. Kar, "A multi charging station for electric vehicles and its utilization for load management and the grid support," *IEEE Trans. Smart Grid*, vol. 4, no. 2, pp. 1026–1037, Jun. 2013.
[18] X. Xie, et al. "Relaxed control design of discrete-time Takagi-Sugeno fuzzy systems: An event-triggered real-time scheduling approach," *IEEE Transactions on Systems, Man, and Cybernetics: Systems*, 2017.
[19] Y. Nakamura, et al. "Voltage Regulation Utilizing Electric Vehicle Rapid Chargers in a Distribution System," *Electrical Engineering in Japan*, vol. 204, no .3, pp. 21-30, 2018.
[20] J. Yong, et al. "Bi-directional electric vehicle fast charging station with novel reactive power compensation for voltage regulation," *International Journal of Electrical Power & Energy Systems*, vol. 64, pp. 300-310, Jan. 2015.
[21] S. U. Khan, et al. "Energy Management Scheme for an EV Smart Charger V2G/G2V Application with an EV Power Allocation Technique and Voltage Regulation," *Applied Sciences*, vol. 8, no .4, pp. 648, Apr. 2018.
[22] W. Su, et al. "Model predictive control-based power dispatch for distribution system considering plug-in electric vehicle uncertainty," *Electric Power Systems Research*, vol. 106, pp. 29-35, Jan. 2014.
[23] H. S. V. S. Kumar Nunna and S. Doolla, "Energy management in microgrids using demand response and distributed storage—a multiagent approach," *IEEE Trans. Power Delivery*, vol. 28, no. 2, pp. 939-947, Feb. 2013.
[24] F. Guo, et al. "Distributed secondary voltage and frequency restoration control of droop-controlled inverter-based microgrids," *IEEE Trans. Industrial Electronics*, vol. 62, no .7, pp. 4355-4364, Jul. 2015.
[25] Y. Wang, et al. "Aggregated Energy Storage for Power System Frequency Control: A Finite-Time Consensus Approach," *IEEE Trans. Smart Grid*, 2018.
[26] Q. Li, et al. "Consensus-Based Distributed Economic Dispatch Control Method in Power Systems," *IEEE Transactions on Smart Grid*, 2017.
[27] X. J. Li, D. Hui, and X. K. Lai, "Battery energy storage station (BESS)-based smoothing control of photovoltaic (PV) and wind power generation fluctuations," *IEEE Trans. Sustainable Energy*, vol. 4, no. 2, pp. 464-473, Mar. 2013.
[28] Rahmoun and H. Biechl, "Modelling of Li-ion batteries using equivalent circuit diagrams," *Electrical Review*, pp. 152-156, Jan. 2012.
[29] Charging a Nissan Leaf (24kWh). https://newmotion.com/en/drive-electric/car/nissan-leaf-24kwh.
[30] J. G. Pinto, V. Monteiro, H. Goncalves, and J. L. Afonso, "Onboard reconfigurable battery charger for electric vehicles with traction-to-auxiliary mode," *IEEE Trans. Vehicular Technology*, vol. 63, no. 3, pp. 1104-1116, Sep. 2013.
[31] G. Mokhtari, A. Ghosh, G. Nourbakhsh, and G. Ledwich, "Smart robust resources control in LV network to deal with voltage rise issue," *IEEE Trans. Sustainable Energy*, vol. 4, no. 4, pp. 1043-1050, Oct. 2013.
[32] J. Jardini, C. M. V. Tahan, M. R. Gouvea, A. S. Un, et. al., "Daily load profiles for residential, commercial and industrial low voltage consumers," *IEEE Trans. Power Delivery*, vol. 15, no. 1, pp. 375-380, Jan. 2000.